energies

MDPI

Article

Piezoelectric Energy Harvesting from Roadways under Open-Traffic Conditions: Analysis and Optimization with Scaling Law Method

Yangyang Zhang [1,*], Qi Lai [1], Ji Wang [1] and Chaofeng Lü [1,2]

[1] Faculty of Mechanical Engineer and Mechanics, Ningbo University, Ningbo 315211, China; laiqi45@163.com (Q.L.); wangji@nbu.edu.cn (J.W.); lucf@zju.edu.cn (C.L.)
[2] Department of Civil Engineering, Zhejiang University, Hangzhou 310058, China
* Correspondence: zhangyangyang@nbu.edu.cn

Abstract: Piezoelectric energy harvesting from roadways, which converts ambient vibration energy of roads into electric energy, has a wide range of potential applications in intelligent transportation systems. On-site open-traffic tests revealed that energy harvested by piezoelectric energy harvester (PEH) units embedded in roadways is far less than the value in laboratories, which may be because the parameters of traffic flow load (frequency, distribution, wave shape, etc.) and the road structure are significantly different from the pre-established conditions in laboratories or even on-site tests with only one vehicle passing. To address this issue, an analytical model for piezoelectric energy harvesting from roadways under open-traffic conditions was proposed to examine the mechanical response of the road structure and the electrical performance of the stack PEH units embedded in the road. The influence of all parameters in the energy-harvesting system was then obtained with the scaling law method, revealing that the energy harvested by PEH units is determined by the energy coefficient, the system's intrinsic parameter, normalized parameters of roadways, and the normalized embedded position of PEH units. It is found that that the energy-harvesting system's intrinsic parameter should be approximately 0.8 to ensure maximum energy-harvesting efficiency. Meanwhile, the pavement with lower bending stiffness and higher linear density while the foundation with small stiffness and smaller damping coefficient would be more suitable for energy harvesting. Furthermore, the lateral embedded position of PEH units should be carefully chosen, since the units embedded in an optimal position can harvest three times more than that embedded in other positions. The concise criteria presented in this study will be used as a reference not only for material selection, dimension optimization, and embedded positions determination of PEH units but also for choosing of the optimal roadways to achieve maximum piezoelectric energy harvesting efficiency under open-traffic conditions.

Keywords: piezoelectric energy harvesting; intelligent pavement; scaling law method

check for updates

Citation: Zhang, Y.; Lai, Q.; Wang, J.; Lü, C. Piezoelectric Energy Harvesting from Roadways under Open-Traffic Conditions: Analysis and Optimization with Scaling Law Method. *Energies* **2022**, *15*, 3395. https://doi.org/10.3390/en15093395

Academic Editor: Abdelali El Aroudi

Received: 26 March 2022
Accepted: 30 April 2022
Published: 6 May 2022

Publisher's Note: MDPI stays neutral with regard to jurisdictional claims in published maps and institutional affiliations.

Copyright: © 2022 by the authors. Licensee MDPI, Basel, Switzerland. This article is an open access article distributed under the terms and conditions of the Creative Commons Attribution (CC BY) license (https://creativecommons.org/licenses/by/4.0/).

1. Introduction

With the increase in global highway mileage and car ownership, considerable vibration energy is accumulated in the roadways and then dissipated in vain. Harvesting the ubiquitous vibration energy from roads would be potential to provide electricity for sensors embedded in infrastructures and for traffic auxiliary facilities such as street lights and signage. This would be of special importance when grid power supply and battery replacement are inconvenient [1–4].

Piezoelectric energy harvesters (PEHs) have attracted extensive attention both from the industry and research community in the recent yeas, because they are easily fabricated, deployable for all kinds of roads, and independent from weather conditions [5]. In 2008, Innowattech, an Israeli company, fabricated a road-capable PEH and then carried out

on-site tests [6,7]. It claimed that for a single lane, 1 km-long PEH, as high as 200 kWh electricity can be harvested in one hour. Nevertheless, neither detailed information regarding structural design nor experimental raw data can be found about the PEH. Afterward, PEHs with different piezoelectric materials [8–10], structural design strategies [11–26], package methods [27,28], series-parallel connections [29,30], energy-harvesting circuits [31,32], etc. are extensively investigated with enormous carefully designed laboratory tests, theoretical analyses [33–36], and finite element simulations [37,38]. These research studies have greatly promoted the development of PEHs in laboratory experiments and thus lay a solid foundation for future field studies.

Several research groups have conducted field tests in recent years. Wang et al. carried out a series of on-site experiments since 2016 to investigate the electrical performance of PEH units under vehicles with different axle loads and driving speeds, and four LED Chinese characters were lit up successfully with the harvested energy [39–41]. Hwang et al. fabricated a kind of road-capable PEHs, which provided sufficient electric energy for a temperature sensor to measure data 14 times in 16 s and then transmitted the data wirelessly [42]. Song et al. installed a PEH in a speed bump, and a 10,000 μF capacitor was charged up to 6 V when a vehicle passed the PEH nine times at 30 km/h [43]. Chen et al. demonstrated an innovative roadway PEH by incorporating a compression-to-compression force amplification mechanism to achieve a high energy density [44]. Recently, Hong et al. developed a uniform stress distribution road piezoelectric generator, which can provide sufficient energy to charge a mobile phone battery for 53 s when a compact vehicle compressed 25 units at a speed of 100 km/h [45]. These on-site experiments studied the scenario that only one vehicle passes this PEH.

Nevertheless, under real traffic conditions, the vehicles' types, axle loads, traffic speeds, and following distances would change with certain randomness (Figure 1). To evaluate the performance of PEHs under open-traffic conditions, Wang et al. installed a piezoelectric micro-energy collection-storage system in roadways, and the harvested electric energy was used to charge a capacitor. The results showed that only 76 mJ electrical energy was stored in the capacitor after 1200 random automobiles passed this PEH in 3 h [46].

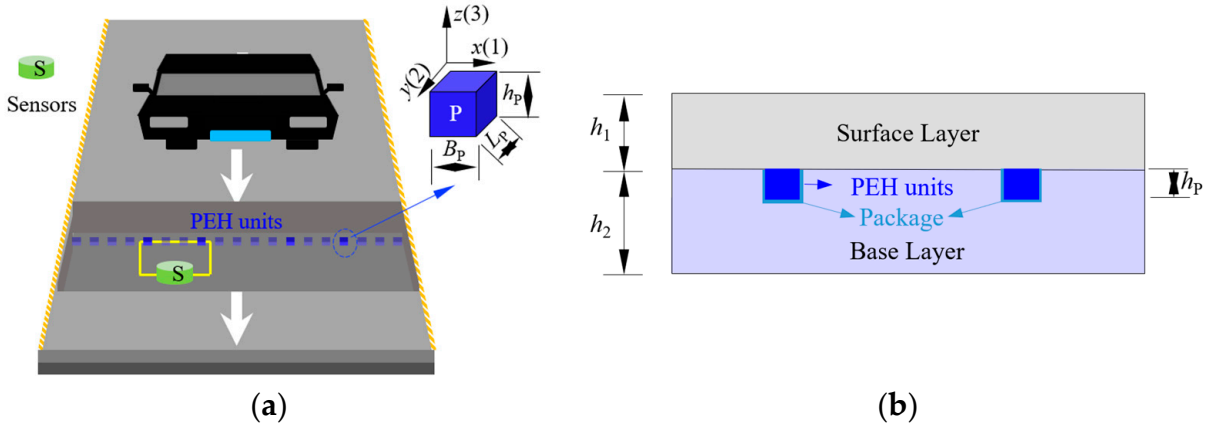


Figure 1. Schematic illustration of piezoelectric energy harvesting from pavement. (**a**) Piezoelectric energy harvester (PEH) units embedded in the road. (**b**) Transverse section view.

These on-site experiments fully validated the feasibility of harvesting vibration energy of the pavement structure with PEHs to power low-energy electronics. Nevertheless, when comparing the energy gathered in on-site tests with that in laboratory experiments, it would be found that the energy-harvesting efficiency drops dramatically in on-site tests, especially under open-traffic conditions. This would be because the parameters of traffic load (frequency, load distribution, waveform, etc.) and the roadways (material, structure, etc.) would be significantly different from the simulation conditions in laboratories, and the influence of these huge differences have yet not been clarified in the research to date.

To fill this research gap, a theoretical model is proposed to examine the electric performance of PEH units under open-traffic conditions. The structure of the roadway is simplified as a composite beam resting on the Kelvin–Voigt foundation, and the distribution of the traffic flow load along the transverse direction is simplified as a pair of parabolas, whereas the traffic load along the longitudinal direction is equalized as a series of half-cycle sinusoidal pulses, as shown in detail in Section 2. Then, the scaling law method is applied to analyze this system (Section 3), and the effects of four combined normalized parameters that can fully determine the amount of energy harvested by PEH units under traffic load are examined systematically (Section 4). The objective of this present study is to identify criteria to guide the design and arrangement of PEH units as well as the selection of proper roadways for achieving maximum energy-harvesting efficiency under open-traffic conditions.

2. Electromechanical Modeling

2.1. Mechanical Response of Roadways under Traffic Flow Load

The road structure under traffic load can be modeled as a composite beam resting on the Kelvin–Voigt foundation (Figure 2), and the corresponding governing equation can be expressed as [33–36]

$$D\frac{\partial^4 w(x,t)}{\partial x^4} + \rho\frac{\partial^2 w(x,t)}{\partial t^2} + C\frac{\partial w(x,t)}{\partial t} + Kw(x,t) = q(x,t), \quad (1)$$

where $w(x,t)$ is the deflection of the composite beam, D and ρ are the bending stiffness and linear density of the composite beam, C and K are the damping coefficient and stiffness of the foundation, and $q(x,t)$ stands for the distribution of traffic load.

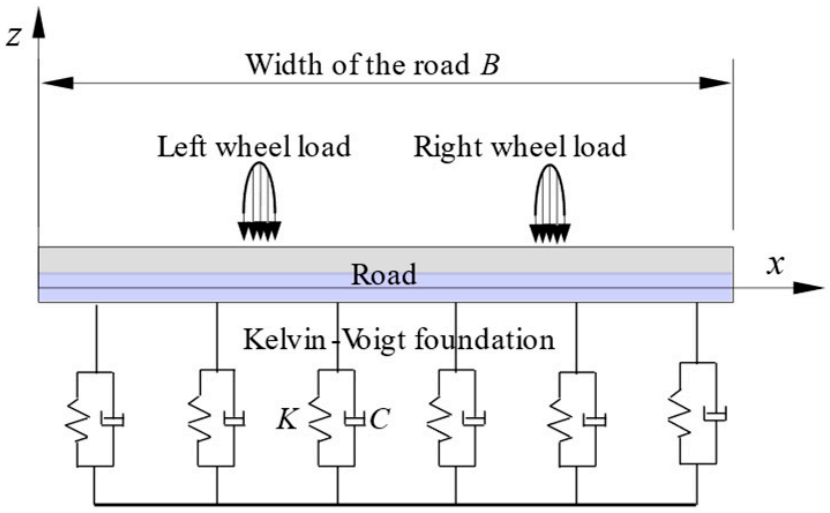


Figure 2. Schematic illustration of the road under traffic load.

The traffic load $q(x,t)$ can be described as follows:

$$q(x,t) = q_0 f_B(x) f_L(t), \quad (2)$$

where q_0 is the amplitude of traffic load, which is directly depending on the axle loads of the vehicle; $f_B(x)$ stands for the distribution of traffic load along the width direction of the road; and $f_L(t)$ stands for the time-history of traffic load along the driving direction (Figure 2).

The shape of the load distribution of a single tire applied on the pavements can be simplified as a parabola line [8]. Then, the distribution of traffic load along the width direction can be described as follows:

$$f_{\mathrm{B}}(x) = \begin{cases} -4(x - x_{\mathrm{C}} - B_{\mathrm{V}}/2)^2/B_{\mathrm{C}}^2 + 1 & x \in \left[x_{\mathrm{C}} + \frac{B_{\mathrm{V}}-B_{\mathrm{C}}}{2},\ x_{\mathrm{C}} + \frac{B_{\mathrm{V}}+B_{\mathrm{C}}}{2}\right] \\ -4(x - x_{\mathrm{C}} + B_{\mathrm{V}}/2)^2/B_{\mathrm{C}}^2 + 1 & x \in \left[x_{\mathrm{C}} - \frac{B_{\mathrm{V}}+B_{\mathrm{C}}}{2},\ x_{\mathrm{C}} - \frac{B_{\mathrm{V}}-B_{\mathrm{C}}}{2}\right] \\ 0 & \text{other} \end{cases}, \quad (3)$$

in which x_{C} stands for the wheel path position, i.e., the distance from the center of the vehicle to the roadside; B_{V} stands for the track width, i.e., the lateral distance between the centerlines of the two tires; and B_{C} stands for the width of the contact area between tires and roads (Figure 3a).

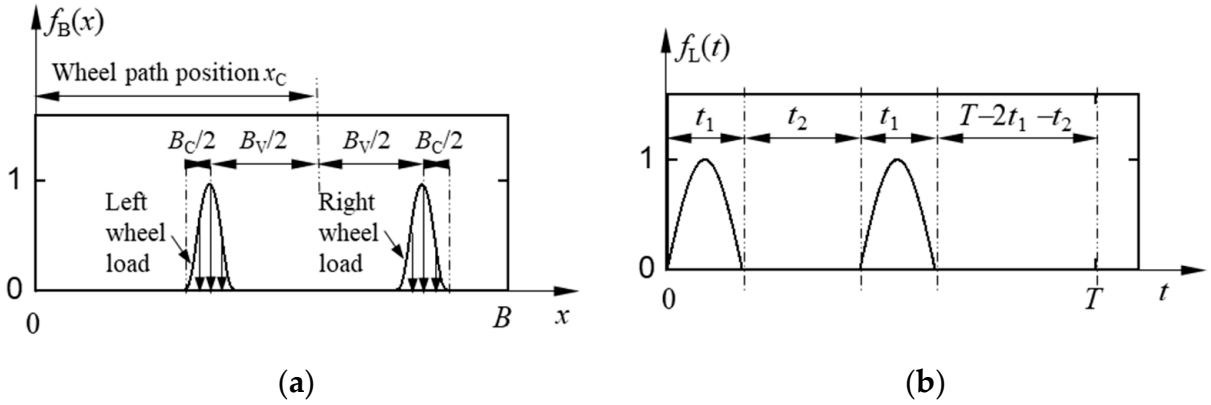


Figure 3. Schematic illustration of the traffic load. (**a**) Distribution of traffic load along the width direction of the road. (**b**) Time-history of traffic load along the driving direction.

The time-history waveform of the traffic load applied by a single tire on a PEH can be simplified as a half-cycle sinusoidal pulse $f(t) = \sin(\omega t)$, in which $t \in [0, \pi/\omega]$. Thus, for a vehicle with speed v and wheelbase L_{W} (the distance between the front and rear axles) that passes the PEH, the time-history of traffic load along the driving direction can be obtained as

$$f_{\mathrm{L}}(t) = \begin{cases} \sin(\pi t/t_1) & t \in [0, t_1] \\ \sin[\pi(t - t_1 - t_2)/t_1] & t \in [t_1 + t_2, 2t_1 + t_2] \\ 0 & \text{other} \end{cases}, \quad (4)$$

in which $t_1 = (L_{\mathrm{C}} + L_{\mathrm{P}})/v$, and $t_2 = L_{\mathrm{W}}/v$. Here, L_{C} stands for the length of the contact area between tires and roads, and L_{P} stands for the length of a PEH unit. The following distance, that is, the distance between two consecutive vehicles traveling along the same direction, is denoted as L_{S}, and then, the period T of the traffic load can be expressed as $T = (L_{\mathrm{W}} + L_{\mathrm{S}})/v$; thus, $f_{\mathrm{L}}(t) = f_{\mathrm{L}}(t + T)$ (Figure 3b).

Substituting Equations (2)–(4) into Equation (1), the deflection of the composite beam $w(x, t)$ can be obtained readily.

2.2. Electromechanical Modeling of PEHs

Previous research studies suggest that multilayer stack structural PEHs are of good durability under traffic load and also convenient for on-site installation [47–49]. Here, this type of PEHs is used as a typical example in the forthcoming analysis. The PEHs embedded in the pavement would endure stress and strain when traffic flow load is applied on the road. Then, according to the constitutive relationship of piezoelectric material, the accumulated charge of the ith PEH (dimension: $L_{\mathrm{P}} \times B_{\mathrm{P}} \times h_{\mathrm{P}}$) can be obtained as

$$Q_i(t) = C_{\mathrm{P}} V_i - \alpha \frac{\partial w^2(x, t)}{\partial x^2}\Big|_{x=x_i}. \quad (5)$$

where V_i is the voltage drop across the PEH, $C_P = \frac{L_P B_P}{h_P}\left(\varepsilon_{33} - \frac{2d_{31}^2}{s_{11}+s_{12}}\right)$ is the equivalent capacitance of the PEH unit, and $\alpha = \frac{L_P B_P d_{31} h_c Y_2}{(s_{11}+s_{12})Y_P}$ is the equivalent force factor. Here, d_{31}, ε_{33}, s_{11}, and s_{12} are the piezoelectric constant, dielectric constant, and elastic constants of the piezoelectric material, respectively; x_i is the embedded position of the ith PHE unit; Y_2 and Y_P are the Young's modulus of the base layer of road and piezoelectric material; and h_c is the distance from the center of piezoelectric layer to the neutral axis of the whole composite cross-section.

When the PEH unit is connected to a resistor with resistance R, the current in this circuit would be $I_i = -\mathrm{d}Q_i(t)/\mathrm{d}t = V_i/R$, and then, the governing equation for this circuit can be written as follows:

$$\frac{\mathrm{d}V_i(t)}{\mathrm{d}t} + \frac{V_i(t)}{RC_P} = \frac{\alpha}{C_P}\frac{\partial w^3(x,t)}{\partial x^2 \partial t}\Big|_{x=x_i}. \tag{6}$$

With the initial condition $V_i(0) = 0$, the voltage across the ith PEH unit can be derived as

$$V_i(t) = \frac{\alpha}{C_P}\exp\left(-\frac{t}{RC_P}\right)\int_0^t \exp\left(\frac{t'}{RC_P}\right)\left[\frac{\partial w^3(x,t)}{\partial x^2 \partial t}\Big|_{x=x_i}\right]\mathrm{d}t' \tag{7}$$

So, when the wheel path position of a vehicle is x_C, the energy harvested by the ith PEH in a period T as the vehicle passes can be obtained as

$$\widehat{\mathrm{E}}_i(x_C) = \left[\int_0^T V_i^2(t)\mathrm{d}t\right]/R \tag{8}$$

According to the standard <BS 5400, Steel, Concrete and Composite Bridges-Part 10: Code of Practice for Fatigue>, which is published by the British Standards Institution in 1980, the distribution of the wheel path position x_C follows a Gaussian distribution, i.e., $p(x_C) \sim \mathrm{N}(\mu, \sigma^2)$. Thus, considering the lateral wheel path distribution, the energy harvested by the ith PEH in a period T can be obtained as

$$E_i = \int_{\min(x_C)}^{\max(x_C)} \widehat{\mathrm{E}}_i(x_C)p(x_C)\mathrm{d}x_C \tag{9}$$

3. Scaling Law Analysis

From the above-mentioned theoretical model, it can be seen that as many as 24 parameters are contained in the piezoelectric energy-harvesting system under traffic flow load. There are eight traffic flow load parameters, i.e., the amplitude of traffic load q_0, wheel path position x_C, track width B_V, wheelbase L_W, following distance L_S, traffic speed v, the length L_C and width B_C of the contact area between tires and roads. There are also eight road material and structure parameters, i.e., thickness, density and modulus of the surface layer and base layer of the road, the stiffness K, and damping coefficient C of foundation. The total number of the parameters of PEH units is also 8, and these parameters are the size (L_P, B_P, and h_P), piezoelectric constant d_{31}, dielectric constant ε_{33}, elastic constants (s_{11} and s_{12}), and the embedded position x_i. All these parameters would influence the energy-harvesting efficiency of the piezoelectric energy harvesting system. The traditional approach to examine the influence of these parameters on the energy-harvesting efficiency is based on single parameter analysis, which requires other parameters to be fixed when examining the influence of a concerned parameter. This approach is effective for a simple system but would be insufficient for a complex system, since it is unable to provide a comprehensive understanding of the interaction between these parameters in the system. By contrast, based on the deep understanding about the whole system, the scaling law analysis can provide a comprehensive understanding of the relation between these parameters.

Through in-depth analysis of each equation in the piezoelectric energy-harvesting system, the following dimensionless parameters are selected for the scaling law analysis.

The normalized lateral embedded position of a PEH unit $\overline{x}$ is defined as $\overline{x} = x/B$, in which B is the width of the road; then, the lateral distribution of traffic load along the width of road can be normalized as

$$\overline{f}_{\mathrm{B}}(\overline{x}) = \begin{cases} -\left(\overline{x} - \frac{x_{\mathrm{C}}}{B} - \frac{B_{\mathrm{V}}}{2B}\right)^2 \left(\frac{2B}{B_{\mathrm{C}}}\right)^2 + 1 & \overline{x} \in \left[\frac{x_{\mathrm{C}}}{B} + \frac{B_{\mathrm{V}}}{2B} - \frac{B_{\mathrm{C}}}{2B},\ \frac{x_{\mathrm{C}}}{B} + \frac{B_{\mathrm{V}}}{2B} + \frac{B_{\mathrm{C}}}{2B}\right] \\ -\left(\overline{x} - \frac{x_{\mathrm{C}}}{B} + \frac{B_{\mathrm{V}}}{2B}\right)^2 \left(\frac{2B}{B_{\mathrm{C}}}\right)^2 + 1 & \overline{x} \in \left[\frac{x_{\mathrm{C}}}{B} - \frac{B_{\mathrm{V}}}{2B} - \frac{B_{\mathrm{C}}}{2B},\ \frac{x_{\mathrm{C}}}{B} - \frac{B_{\mathrm{V}}}{2B} + \frac{B_{\mathrm{C}}}{2B}\right] \\ 0 & \text{other} \end{cases} \tag{10}$$

Normalized time $\overline{t}$ is defined as $\overline{t} = t/t_1$, in which $t_1 = (L_{\mathrm{C}} + L_{\mathrm{P}})/v$ is the time needed for a single tire to pass a PEH unit, as aforementioned. Then, the time-history of traffic load along the driving direction can be normalized as

$$\overline{f}_{\mathrm{L}}(\overline{t}) = \begin{cases} \sin(\pi\overline{t}) & t \in [0, 1] \\ \sin\left[\pi\left(\overline{t} - 1 - t_2/t_1\right)\right] & t \in [1 + t_2/t_1, 2 + t_2/t_1] \\ 0 & \text{other} \end{cases} \tag{11}$$

Normalized parameters $\overline{w} = \frac{wD}{q_0 B^4}$, $\overline{\rho} = \frac{\rho B^4}{D t_1^2}$, $\overline{C} = \frac{CB^4}{Dt_1}$, and $\overline{K} = \frac{KB^4}{D}$ are defined and then substituted into Equation (1), and the governing equation for the vibration of the roadway under traffic flow load can be rewritten as

$$\frac{\partial^4 \overline{w}(\overline{x}, \overline{t})}{\partial \overline{x}^4} + \overline{\rho}\frac{\partial^2 \overline{w}(\overline{x}, \overline{t})}{\partial \overline{t}^2} + \overline{C}\frac{\partial \overline{w}(\overline{x}, \overline{t})}{\partial \overline{t}} + \overline{K}\overline{w}(\overline{x}, \overline{t}) = \overline{f}_{\mathrm{B}}(\overline{x})\overline{f}_{\mathrm{L}}(\overline{t}) \tag{12}$$

The normalized output voltage of the ith PEH unit $\overline{V}_i$ can be defined as $\overline{V}_i = V_i/V_0$, in which $V_0 = \frac{\alpha}{C_{\mathrm{P}}}\frac{q_0 B^2}{D}$; then, $\overline{V}_i$ can be derived as

$$\overline{V}_i(\overline{t}) = \pi \exp\left(-\frac{\pi\overline{t}}{R\omega C_{\mathrm{P}}}\right) \int_0^{\overline{t}} \exp\left(\frac{\pi\overline{t'}}{R\omega C_{\mathrm{P}}}\right) \left[\frac{\partial \overline{w}^3(\overline{x}, \overline{t})}{\partial \overline{x}^2 \partial \overline{t}}\Big|_{\overline{x}=\overline{x}_i}\right] \mathrm{d}\overline{t'} \tag{13}$$

in which $\omega = \pi/t_1$.

The normalized energy harvested by the ith PEH unit $\overline{E}_i$ can be defined as $\overline{E}_i = E_i/E_{\mathrm{eff0}}$. Here, $E_{\mathrm{eff0}} = \alpha^2\left(q_0 B^2/D\right)^2/C_{\mathrm{P}}$ is the energy coefficient. Then, $\overline{E}_i$ can be obtained as

$$\overline{E}_{\mathrm{i}} = \overline{E}_{\mathrm{i}}\left(R\omega C_{\mathrm{P}}, \overline{K}, \overline{C}, \overline{\rho}, \overline{x}_i\right) \tag{14}$$

4. Results and Optimization Criteria

From Equation (14), it can be seen that the energy E_i harvested by a PEH unit in a period T is linear with the energy coefficient E_{eff0}, and it is also influenced by the system's intrinsic parameter $R\omega C_{\mathrm{P}}$, the normalized stiffness $\overline{K}$ and the normalized damping coefficient $\overline{C}$ of the foundation, the normalized linear density $\overline{\rho}$ of the pavement, and also the unit's lateral embedded position $\overline{x}_i = x_i/B$.

4.1. Influence of Energy Coefficient E_{eff0}

Substitute the expressions of α and C_{P} into $E_{\mathrm{eff0}} = \alpha^2\left(q_0 B^2/D\right)^2/C_{\mathrm{P}}$, the energy coefficient E_{eff0} can be rewritten as

$$E_{\mathrm{eff0}} = (L_{\mathrm{P}} B_{\mathrm{P}} h_{\mathrm{P}}) q_0^2 \frac{B^4}{D^2} \frac{Y_2^2}{Y_{\mathrm{P}}^2} h_{\mathrm{c}}^2 \frac{d_{31}^2}{\left[\varepsilon_{33} - 2d_{31}^2/(s_{11} + s_{12})\right](s_{11} + s_{12})^2}, \tag{15}$$

Equation (15) shows that when normalized energy $\overline{E}_{\mathrm{i}}$ is fixed, the energy harvested by PEH units would be linear to the energy coefficient E_{eff0}. This would arrive at the following conclusions. ① Energy harvested by the PEH units is linear to the total volume of piezoelectric material ($V_{\mathrm{P}} = L_{\mathrm{P}} B_{\mathrm{P}} h_{\mathrm{P}}$). Therefore, when evaluating the energy efficiency of different PEHs, the energy harvested per unit volume piezoelectric material should be applied to compare. ② Energy harvested by PEH units is directly proportional to the square of the amplitude of traffic load, i.e., $E_{\mathrm{i}} \propto q_0^2$. ③ Energy harvested by PEH units is linear to the combination coefficient $\frac{B^4}{D^2}\frac{Y_2^2}{Y_{\mathrm{P}}^2}$ of the pavement structure. This means the larger the ratio of the fourth power of the road's width to the square of the road's bending stiffness (D^2), the larger the ratio of the road's base layer's Young's modulus Y_2 to the piezoelectric material's Young's modulus Y_{P}; then, the PEH units embedded in the road can harvest energy more efficiently. This relationship can guide the choice of suitable roadways for embedding PEH units. ④ Energy harvested by PEH units is directly proportional to the square of the distance from the center of the piezoelectric layer to the neutral axis of the whole composite cross-section, i.e., $E_{\mathrm{i}} \propto h_{\mathrm{c}}^2$. This relationship can be used to determine the embedded depth of PEH units. ⑤ The larger the combination coefficient $d_{31}^2 / \left[\varepsilon_{33} - 2d_{31}^2/(s_{11}+s_{12})\right] / (s_{11}+s_{12})^2$ of the piezoelectric material, the higher the energy-harvesting efficiency. This relationship could be used as a guideline for choosing proper piezoelectric material.

4.2. Influence of System's Intrinsic Parameter $R\omega C_{\mathrm{P}}$

In the piezoelectric energy-harvesting systems, $R\omega C_{\mathrm{P}}$ is an intrinsic normalized parameter that denotes the effect of matching between the external resistance R, the equivalent capacitance of the PHE and the frequency of the excitation ω. In practical applications, the external resistance R of the electronics embedded in the pavement, the excitation frequency ω of the traffic load, and the equivalent capacitance of the PHE C_{P} codetermine the value of $R\omega C_{\mathrm{P}}$. For a typical road [50] with common traffic speed $v = 20$ m/s, the normalized parameters can be calculated as $\overline{\rho} = \frac{\rho B^4}{D t_1^2} = 105$, $\overline{C} = \frac{C B^4}{D t_1} = 375$, $\overline{K} = \frac{K B^4}{D} = 1480$. Then, when the parameters of roads and traffic speed are changed, the $\overline{\rho}$, $\overline{C}$, $\overline{K}$ would be changed accordingly. Therefore, the variance of the values of $\overline{\rho}$, $\overline{C}$, and $\overline{K}$ can cover different kinds of roads under various traffic speeds. The influence of the system's intrinsic parameter $R\omega C_{\mathrm{P}}$ on the energy-harvesting efficiency is investigated under four typical types of roads (Figure 4). Here, the vertical coordinate $\overline{E} = \sum_{i=1}^{N} \overline{E}_i$ denotes the energy harvested by all of the PEH units embedded in the pavement. In other words, the total length of these units equals the overall width of the pavement. For all these four distinct kinds of roads, the optimal $R\omega C_{\mathrm{P}}$, which is corresponding to the maximum harvested energy, is 0.75, 0.80, 0.85, 0.75, respectively (as shown by the four lines from up to down in Figure 4). Thus, in practical application, it is acceptable to make $R\omega C_{\mathrm{P}} = 0.8$, since this can guarantee 95% of the highest energy harvesting efficiency for the four different road conditions (Figure 4). Generally, there are two ways to satisfy this criterion. ① Adjust the external impedance R. Once the PEH unit is designed, the equivalent capacitance C_{P} of the device is determined. Then, the external impedance R should be adjusted according to the traffic speeds (such as expressway with high traffic speed, urban roads with low traffic speed) to ensure $R\omega C_{\mathrm{P}} = 0.8$, since $\omega = \pi v/(L_{\mathrm{C}} + L_{\mathrm{P}})$. ② Adjust the design of PEH units. Under certain circumstances, the external impedance R of the electronics may be unchangeable. So, the equivalent capacitance C_{P} of the PEH units should be adjusted to make $R\omega C_{\mathrm{P}} = 0.8$. Since $C_{\mathrm{P}} = \frac{L_{\mathrm{P}} B_{\mathrm{P}}}{h_{\mathrm{P}}}\left(\varepsilon_{33} - \frac{2d_{31}^2}{s_{11}+s_{12}}\right)$, the dimension of PHE ($L_{\mathrm{P}}$, B_{P}, h_{P}) can be tuned to make C_{P} satisfy this criterion.

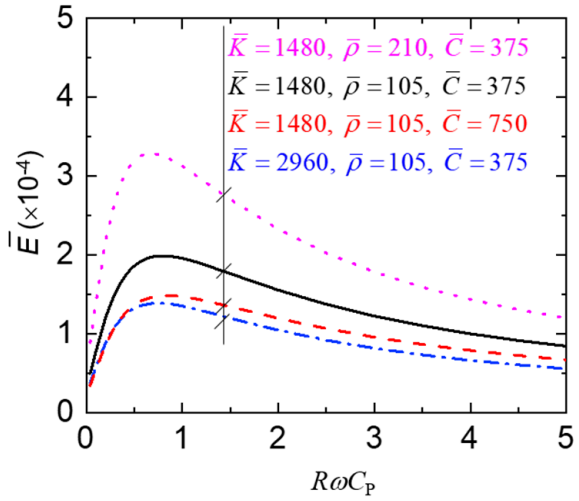


Figure 4. Influence of the piezoelectric energy harvesting system's intrinsic parameter $R\omega C_P$ on the normalized energy $\overline{E}$.

4.3. Influence of Normalized Parameters ($\overline{K}$, $\overline{C}$, and $\overline{\rho}$) of Roads

The influence of normalized foundation stiffness $\overline{K}$ of the foundation is evaluated for four typical roads with varied normalized linear density $\overline{\rho}$ and damping coefficient $\overline{C}$ (Figure 5a). The results show that the normalized harvested $\overline{E}$ would decrease with the increase in the normalized foundation stiffness $\overline{K}$ for all these four different roads. This is because the strain of piezoelectric material would be reduced with the increasing of the normalized foundation stiffness $\overline{K}$, whereas the traffic load and other parameters of the road are unchanged. Thus, the roadways with lower foundation stiffness are preferred to achieve higher energy harvesting efficiency.

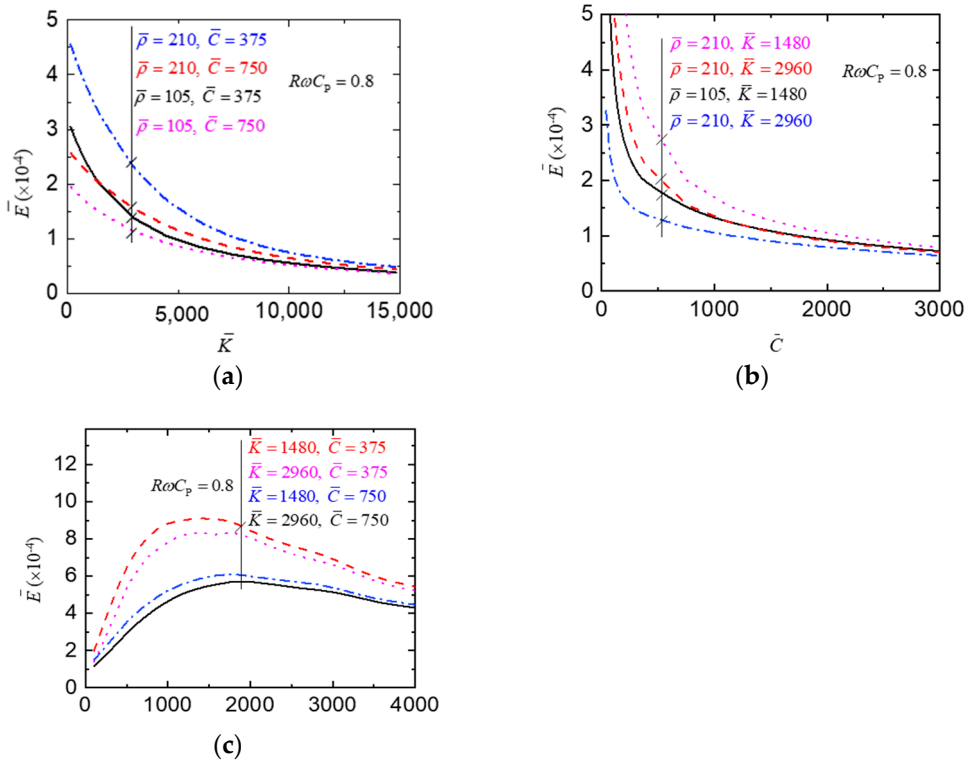


Figure 5. Influence of the normalized parameters of pavements ($\overline{K}$, $\overline{C}$, $\overline{\rho}$) on the normalized energy $\overline{E}$. (**a**) Influence of normalized foundation stiffness $\overline{K}$. (**b**) Influence of normalized foundation damping coefficient $\overline{C}$. (**c**) Influence of normalized linear density $\overline{\rho}$.

The influence of the normalized damping coefficient $\overline{C}$ of the foundation is also investigated under four typical roads (Figure 5b). The results show that the normalized harvested $\overline{E}$ would decrease with the increase in the normalized foundation damping coefficient $\overline{C}$ for all these four different roads. This is because the vibration of PEH units would decay more quickly if the damping coefficient of the foundation is larger; consequently, the electric output power of PEH units would also decrease more quickly, resulting in the decease of the energy harvested by PEH units. Thus, the roads with lower foundation damping coefficients are preferred to maximize higher energy harvesting efficiency.

The influence of the pavement's normalized linear density $\overline{\rho}$ is investigated under four typical roads similarly (Figure 5c). The results reveal that the harvested energy of PEH units would increase first and then decrease with the increasing normalized linear density $\overline{\rho}$. This is because the fundamental natural frequency ($\omega_{\mathrm{n}} = \sqrt{(1+\overline{K})/\overline{\rho}}$) would decrease and normalized excitation frequency $s = \omega/\omega_{\mathrm{n}}$ would increase with the increasing of normalized linear density $\overline{\rho}$. From the frequency response function $H(s)$ in basic vibration theories, it can be seen that the response of the system would increase first and then decrease with the normalized excitation frequency s, which would cause the energy gathered by PEH units to change in the same way.

In practical conditions, the traffic condition with smaller $\overline{K}$, smaller $\overline{C}$ and moderate $\overline{\rho}$ (approximate 1000) would guarantee the highest energy-harvesting efficiency.

4.4. Influence of Normalized Lateral Embedded Position $\overline{x}_i$ of PEH Units

The influence of the normalized lateral embedded position $\overline{x}_i$ of PEH units is investigated under three distinct types of roads, i.e., type 1 with $\overline{\rho} = 270$, $\overline{C} = 1125$, $\overline{K} = 1480$, type 2 with $\overline{\rho} = 60$, $\overline{C} = 750$, $\overline{K} = 1480$, and type 3 with $\overline{\rho} = 30$, $\overline{C} = 375$, $\overline{K} = 1480$, as shown in Figure 6. It can be seen that the PEH units embedded at the middle of the pavement ($\overline{x}_i = 0.5$) could harvest more energy than the units embedded near the wheels ($\overline{x}_i = 0.25, 0.75$) when $\overline{\rho} = 270$, $\overline{C} = 1125$, and $\overline{K} = 1480$. According to the definition of these normalized parameters, it can be known that this would be corresponding to the condition that the velocity of vehicles is relatively high. By contrast, when $\overline{\rho} = 30$, $\overline{C} = 375$, and $\overline{K} = 1480$, which means that the speed of vehicles is relatively low, PEH units embedded near the wheels ($\overline{x}_i = 0.25, 0.75$) would harvest more energy than those embedded at the middle of the pavement ($\overline{x}_i = 0.5$). When $\overline{\rho} = 60$, $\overline{C} = 750$, and $\overline{K} = 1480$, the energy harvested by PEH units embedded at the middle of the pavement would be similar to that embedded near the wheels. In short, the lateral embedded positions of PEH units should be carefully chosen, since the unit embedded at optimal positions would harvest as much as four times that patched at bed locations (Figure 6), and the optimal lateral embedded positions should be adjusted according to the normalized road parameters ($\overline{K}$, $\overline{C}$, and $\overline{\rho}$), which are dependent both on the parameters of roads and the speed of vehicles.

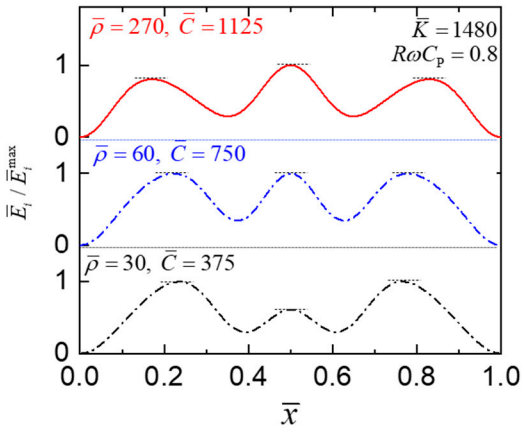


Figure 6. Influence of the normalized embedded position $\overline{x}$ of the piezoelectric energy harvester units on the normalized energy $\overline{E}$.

4.5. Energy Harvested by PEH Units: A Numerical Example

Based on the above calculations, for a typical road ($\overline{\rho} = 105$, $\overline{C} = 375$, and $\overline{K} = 1480$) [50], as a vehicle ($q_0 = 0.7$ MPa) passes with common traffic speed $v = 20$ m/s, the PEH unit (parameters are listed in Table 1) that are embedded in the optimal lateral positions of the pavement can harvest 0.68 mJ. If 1000 such vehicles pass this unit in one hour, then it can be estimated that the energy harvested by the piezoelectric material can achieve as 13,600 J/m^3.

Table 1. Parameters of the PEH units.

Geometry and Material Parameters	Value
Length of a PEH unit, L_P (m)	0.05
Width of a PEH unit, B_P (m)	0.05
Thickness of a PEH unit, h_P (m)	0.02
Piezoelectric constant, d_{31} (C/N)	-2.74×10^{-10}
Dielectric constants, ε_{33} (F/m)	3.98×10^{-8}
Elastic compliances, s_{11} (Pa^{-1})	16.5×10^{-12}
Elastic compliances, s_{12} (Pa^{-1})	-4.78×10^{-12}

5. Conclusions

An integrated electromechanical model incorporating a composite beam resting on the Kelvin–Voigt foundation is proposed to investigate the piezoelectric energy harvesting of pavements under open-traffic conditions, and the electric performance of PEH units embedded in the pavement is theoretically calculated with this model. A concise scaling law is established to reveal the intrinsic relationship between the energy-harvesting efficiency of PEH units and four combined parameters in the system, i.e., the energy coefficient, the energy harvesting system's intrinsic parameter, normalized parameters of roadways, and normalized lateral embedded position of PEH units. The results reveal that the energy-harvesting system's intrinsic parameter should be approximately 0.8 to ensure maximum energy harvesting efficiency. Meanwhile, when the pavement has lower bending stiffness and higher linear density and the foundation has small stiffness and smaller damping coefficient, the roadway would be more suitable for energy harvesting. Furthermore, the optimal lateral embedded position of PEH units should be adjusted with the parameters of roads and traffic speeds. This theoretical model can be used as a reference for material selection, structural optimization, and lateral embedded position determination of PEH units, as well as the selection of the roadway to achieve optimal efficiency for PEHs embedded in pavement under on-site open-traffic conditions.

Author Contributions: Conceptualization, Y.Z. and C.L.; methodology, Y.Z. and Q.L.; writing—original draft preparation, Y.Z. and Q.L.; writing—review and editing, J.W.; supervision, funding acquisition, Y.Z. and C.L. All authors have read and agreed to the published version of the manuscript.

Funding: This research was funded by National Key R & D Program of China (Grant no. 2020YFA0711 700), and the National Natural Science Foundation of China (Grant nos. 11902168, and 11925206).

Institutional Review Board Statement: Not applicable.

Informed Consent Statement: Not applicable.

Data Availability Statement: Not applicable.

Conflicts of Interest: The authors declare no conflict of interest.

References

1. Farinholt, K.; Taylor, S.; Miller, N.; Sifuentes, W.; Moro, E.; Park, G.; Farrar, C.; Flynn, E.; Mascarenas, D.; Todd, M. Energy harvesting and wireless energy transmission for embedded sensor nodes. *Struct. Health Monit.* **2010**, *9*, 269–280. [CrossRef]
2. Wang, H.; Jasim, A.; Chen, X. Energy harvesting technologies in roadway and bridge for different applications—A comprehensive review. *Appl. Energy* **2018**, *212*, 1083–1094. [CrossRef]

3. Roshani, H.; Dessouky, S.; Montoya, A.; Papagiannakis, A.T. Energy harvesting from asphalt pavement roadways vehicle-induced stresses: A feasibility study. *Appl. Energy* **2016**, *182*, 210–218. [CrossRef]
4. Pei, J.Z.; Zhou, B.C.; Lyu, L. E-Road: The largest energy supply of the future? *Appl. Energy.* **2019**, *241*, 174–183. [CrossRef]
5. Gholikhani, M.; Roshani, H.; Dessouky, S.; Papagiannakis, A.T. A critical review of roadway energy harvesting technologies. *Appl. Energy* **2020**, *261*, 114388. [CrossRef]
6. Ahmad, S.; Mujeebu, A.M.; Farooqi, M.A. Energy harvesting from pavements and roadways: A comprehensive review of technologies, materials, and challenges. *Int. J. Energy Res.* **2019**, *43*, 1974–2015. [CrossRef]
7. Qabur, A.; Alshammari, K. A Systematic Review of Energy Harvesting from Roadways by using Piezoelectric Materials Technology. *Innov. Energy Res.* **2018**, *7*, 1–6. [CrossRef]
8. Zhao, H.D.; Ling, J.M.; Yu, J. A comparative analysis of piezoelectric transducers for harvesting energy from asphalt pavement. *J. Ceram. Soc. Jpn.* **2012**, *120*, 317–323. [CrossRef]
9. Lin, L.; Hu, Y.; Xu, C.; Zhang, Y.; Zhang, R.; Wen, X.; Lin Wang, Z. Transparent flexible nanogenerator as self-powered sensor for transportation monitoring. *Nano Energy* **2013**, *2*, 75–81. [CrossRef]
10. Jung, I.; Shin, Y.H.; Kim, S.; Choi, J.Y.; Kang, C.Y. Flexible piezoelectric polymer-based energy harvesting system for roadway applications. *Appl. Energy* **2017**, *197*, 222–229. [CrossRef]
11. Wang, C.H.; Wang, S.; Li, Q.J.; Wang, X.J.; Gao, Z.W.; Zhang, L. Fabrication and performance of a power generation device based on stacked piezoelectric energy-harvesting units for pavements. *Energy Convers. Manag.* **2018**, *163*, 196–207. [CrossRef]
12. Jiang, X.Z.; Li, Y.C.; Li, J.C.; Wang, J.; Yao, J. Piezoelectric energy harvesting from traffic-induced pavement vibrations. *J. Renew. Sustain. Energy* **2014**, *6*, 043110. [CrossRef]
13. Ding, G.; Zhao, X.; Sun, F.; Wang, J. Effect of subgrade on piezoelectric energy harvesting under traffic loads. *Int. J. Pavement Eng.* **2017**, *19*, 661–674. [CrossRef]
14. Papagiannakis, A.T.; Montoya, A.; Dessouky, S.; Helffrich, J. Development and evaluation of piezoelectric prototypes for roadway energy harvesting. *J. Energy Eng.* **2017**, *143*, 04017034. [CrossRef]
15. Roshani, H.; Dessouky, S.; Papagiannakis, A.T.; Montoya, A. Experimental and finite element assessment of three energy harvesting prototypes for roadways. *Innov. Infrastruct. Solut.* **2017**, *2*, 1–12. [CrossRef]
16. Wang, X.F.; Shi, Z.F. Double piezoelectric energy harvesting cell: Modeling and experimental verification. *Smart Mater. Struct.* **2017**, *26*, 065002. [CrossRef]
17. Roshani, H.; Jagtap, P.; Dessouky, S.; Montoya, A.; Papagiannakis, A.T. Theoretical and experimental evaluation of two roadway piezoelectric-based energy harvesting prototypes. *J. Mater. Civ. Eng.* **2018**, *30*, 04017264. [CrossRef]
18. Jasim, A.; Wang, H.; Yesner, G.; Safari, A.; Maher, A. Optimized design of layered bridge transducer for piezoelectric energy harvesting from roadway. *Energy* **2017**, *141*, 1133–1145. [CrossRef]
19. Jasim, A.; Yesner, G.; Wang, H.; Safari, A.; Maher, A.; Basily, B. Laboratory testing and numerical simulation of piezoelectric energy harvester for roadway applications. *Appl. Energy* **2018**, *224*, 438–447. [CrossRef]
20. Dogan, A.; Uchino, K.; Newnham, R.E. Composite piezoelectric transducer with truncated conical endcaps "cymbal". *IEEE Trans. Ultrason. Ferroelectr. Freq. Control.* **1997**, *44*, 597–605. [CrossRef]
21. Moure, A.; Rodríguez, M.A.I.; Rueda, S.H.; Gonzalo, A.; Rubio-Marcos, F.; Cuadros, D.U.; Pérez-Lepe, A.; Fernández, J.F. Feasible integration in asphalt of piezoelectric cymbals for vibration energy harvesting. *Energy Convers. Manag.* **2016**, *112*, 246–253. [CrossRef]
22. Yesner, G.; Jasim, A.; Wang, H.; Basily, B.; Maher, A.; Safari, A. Energy harvesting and evaluation of a novel piezoelectric bridge transducer. *Sens. Actuators A Phys.* **2019**, *285*, 348–354. [CrossRef]
23. Guo, L.K.; Lu, Q. Modeling a new energy harvesting pavement system with experimental verification. *Appl. Energy* **2017**, *208*, 1071–1082. [CrossRef]
24. Guo, L.K.; Lu, Q. Numerical analysis of a new piezoelectric-based energy harvesting pavement system: Lessons from laboratory-based and field-based simulations. *Appl. Energy* **2019**, *235*, 963–977. [CrossRef]
25. Jeon, D.H.; Cho, J.Y.; Jhun, J.P.; Ahn, J.H.; Jeong, S.; Jeong, S.Y.; Kumar, A.; Ryu, C.H.; Hwang, W.; Park, H.; et al. A lever-type piezoelectric energy harvester with deformation-guiding mechanism for electric vehicle charging station on smart road. *Energy* **2021**, *218*, 119540. [CrossRef]
26. Chen, Y.S.; Zhang, H.; Zhang, Y.Y.; Li, C.H.; Yang, Q.; Zheng, H.Y.; Lü, C.F. Mechanical energy harvesting from road pavements under vehicular load using embedded piezoelectric elements. *J. Appl. Mech.* **2016**, *83*, 081001. [CrossRef]
27. Zhang, H.; Huang, K.X.; Zhang, Z.C.; Xiang, T.; Quan, L.W. Piezoelectric energy harvesting from roadways based on pavement compatible package. *J. Appl. Mech.* **2019**, *86*, 091012. [CrossRef]
28. Wang, P.; Cheng, R.; Ding, G.; Wang, J.; Liu, Z.; Zhang, H. Optimized testing of package for stacked piezoelectric energy harvester in roadway applications. *Ferroelectr. Lett. Sect.* **2021**, *48*, 104–116. [CrossRef]
29. Wang, C.H.; Zhao, J.X.; Li, Q.; Li, Y.W. Optimization design and experimental investigation of piezoelectric energy harvesting devices for pavement. *Appl. Energy* **2018**, *229*, 18–30. [CrossRef]
30. Li, C.; Yang, F.; Liu, P.; Fu, C.; Liu, Q.; Zhao, H.; Lin, P. Development and piezoelectric properties of a stack units-based piezoelectric device for roadway application. *Sensors* **2021**, *21*, 7708. [CrossRef]
31. Wu, P.H.; Shu, Y.C. Finite element modeling of electrically rectified piezoelectric energy harvesters. *Smart Mater. Struct.* **2015**, *24*, 094008. [CrossRef]

32. Wu, Y.; Badel, A.; Formosa, F.; Liu, W.; Agbossou, A.E. Piezoelectric vibration energy harvesting by optimized synchronous electric charge extraction. *J. Intell. Mater. Syst. Struct.* **2013**, *24*, 1445–1458. [CrossRef]
33. Xiang, H.J.; Wang, J.J.; Shi, Z.F.; Zhang, Z.W. Theoretical analysis of piezoelectric energy harvesting from traffic induced deformation of pavements. *Smart Mater. Struct.* **2013**, *22*, 095024. [CrossRef]
34. Chen, Y.S.; Zhang, H.; Quan, L.W.; Zhang, Z.C.; Lü, C.F. Theoretical assessment on piezoelectric energy harvesting in smart self-powered asphalt pavements. *J. Vib. Eng. Technol.* **2018**, *6*, 1–10. [CrossRef]
35. Zhang, Y.; Zhang, H.; Lü, C.; Chen, Y.; Wang, J. Piezoelectric energy harvesting from roadway deformation under various traffic flow conditions. *J. Intell. Mater. Syst. Struct.* **2020**, *31*, 1751–1762. [CrossRef]
36. Zhao, X.; Xiang, H.; Shi, Z. Piezoelectric energy harvesting from vehicles induced bending deformation in pavements considering the arrangement of harvesters. *Appl. Math. Model.* **2020**, *77*, 327–340. [CrossRef]
37. Zhao, H.D.; Yu, J.; Ling, J.M. Finite element analysis of cymbal piezoelectric transducers for harvesting energy from asphalt pavement. *J. Ceram. Soc. Jpn.* **2010**, *118*, 909–915. [CrossRef]
38. Cafiso, S.; Cuomo, M.; Graziano, A.D.; Vecchio, C. Experimental analysis for piezoelectric transducers applications into roads pavements. *Adv. Mater. Res.* **2013**, *684*, 253–257. [CrossRef]
39. Xiong, H.C.; Wang, L.B. Piezoelectric energy harvester for public roadway: On-site installation and evaluation. *Appl. Energy* **2016**, *174*, 101–107. [CrossRef]
40. Yang, H.L.; Wang, L.B.; Hou, Y.; Guo, M.; Ye, Z.J.; Tong, X.L.; Wang, D.W. Development in stacked-array-type piezoelectric energy harvester in asphalt pavement. *J. Mater. Civ. Eng.* **2017**, *29*, 04017224. [CrossRef]
41. Yang, H.L.; Wang, L.B.; Zhou, B.; Wei, Y.; Zhao, Q. A preliminary study on the highway piezoelectric power supply system. *Int. J. Pavement Res. Technol.* **2018**, *11*, 168–175. [CrossRef]
42. Hwang, W.; Kim, K.-B.; Cho, J.Y.; Yang, C.H.; Kim, J.H.; Song, G.J.; Song, Y.; Jeon, D.H.; Ahn, J.H.; Hong, S.D.; et al. Watts-level road-compatible piezoelectric energy harvester for a self-powered temperature monitoring system on an actual roadway. *Appl. Energy* **2019**, *243*, 313–320. [CrossRef]
43. Song, G.J.; Kim, K.-B.; Cho, J.Y.; Woo, M.S.; Ahn, J.H.; Eom, J.H.; Ko, S.M.; Yang, C.H.; Hong, S.D.; Jeong, S.Y.; et al. Performance of a speed bump piezoelectric energy harvester for an automatic cellphone charging system. *Appl. Energy* **2019**, *247*, 221–227. [CrossRef]
44. Chen, C.; Xu, T.-B.; Yazdani, A.; Sun, J.-Q. A high density piezoelectric energy harvesting device from highway traffic—System design and road test. *Appl. Energy* **2021**, *299*, 117331. [CrossRef]
45. Hong, S.D.; Ahn, J.H.; Kim, K.-B.; Kim, J.H.; Cho, J.Y.; Woo, M.S.; Song, Y.; Hwang, W.; Jeon, D.H.; Kim, J.; et al. Uniform stress distribution road piezoelectric generator with free-fixed-end type central strike mechanism. *Energy* **2022**, *239*, 121812. [CrossRef]
46. Wang, C.H.; Wang, S.; Gao, Z.W.; Song, Z. Effect evaluation of road piezoelectric micro-energy collection-storage system based on laboratory and on-site tests. *Appl. Energy* **2021**, *287*, 116581. [CrossRef]
47. Duong, L.; Pham, M.T.; Chebanenko, V.; Solovyev, A.; Nguyen, C.V. Finite element modeling and experimental studies of stack-type piezoelectric energy harvester. *Int. J. Appl. Mech.* **2017**, *9*, 1750084. [CrossRef]
48. Zhao, H.D.; Tao, Y.J.; Niu, Y.L.; Ling, J.M. Harvesting energy from asphalt pavement by piezoelectric generator. *J. Wuhan Univ. Technol.-Mater. Sci. Ed.* **2014**, *29*, 933–937. [CrossRef]
49. Wang, C.H.; Wang, S.; Gao, Z.W.; Wang, X.J. Applicability evaluation of embedded piezoelectric energy harvester applied in pavement structures. *Appl. Energy* **2019**, *251*, 113383. [CrossRef]
50. Yang, S.P.; Li, S.H.; Lu, Y.J. Investigation on dynamical interaction between a heavy vehicle and road pavement. *Veh. Syst. Dyns.* **2010**, *48*, 923–944. [CrossRef]